

Analytical Load Displacement Curves of RC Columns under Constant Axial and Cyclic Lateral Loads

M. Rizwan¹, M. T. A. Chaudhary², M. Ilyas¹

1. Department of Civil Engineering, University of Engineering & Technology, Lahore, muhammad.rizwan@wits.ac.za.
2. Al Imam Mohammad Ibn Saud Islamic University, Riyadh, Saudi Arabia, mtariqch@hotmail.com.

Abstract

The cyclic tests of the columns are of practical relevance to the performance of compression members during earthquake loading. The strength, ductility and energy absorption capabilities of RC columns, subjected to cyclic loading, have been estimated by many researchers. These characteristics are not normally inherent in plain concrete but can be achieved by effectively confining columns through transverse reinforcement. An extensive experimental program, in which performance of four RC columns detailed according to provisions of ACI-318-08, was studied in comparison with that of four columns confined by a new proposed technique. Out of total eight, this paper presents performance of three columns which were detailed according to provision of ACI-318-08 and cast with 25 and 32 MPa concrete. The experimentally achieved load-displacement hysteresis and backbone curves of the three columns are presented. Two approaches, which utilize moment-curvature and shear-shear strain relationship of RC columns achieved through Response-2000, have been suggested to draw analytical load-displacement curves of the columns. The experimental and analytical load-displacement curves are found in good agreement. The suggested analytical technique is simple and easy to implement. The technique will be available to the engineers involved in design to estimate capacity of RC columns.

Key Words: RCC columns, hysteretic behaviour, Load-Displacement curves

1. Introduction

Concrete is brittle in nature. The confinement provided in reinforced concrete structural components introduces the properties of ductility, deformability and energy dissipation. These properties have important role to play in seismic performance of RC multistorey buildings. In 1903 increase in axial capacity of a concrete column component was found by using spiral transverse reinforcement [1]. Since then the researchers are focusing to quantify the contribution of confinement to the total strength, so that the strength enhancement can be effectively utilized towards high performance design. In early part of 20th century most of the experimental and modelling work, related to confined concrete, was focused to optimize the value of coefficient of the equivalent fluid pressure used in proposed expressions of its compressive strength [2,3]. With passage of time, it was realized that compressive strength of confined concrete is also influenced by shape, pitch, yield strength and

volumetric ratio of confining and longitudinal reinforcement. Many models considering these factors were proposed. In initial models it was assumed that the confining pressure is uniformly distributed. The assumption was adequate for closely spaced hoops only. Later influence of spacing of transverse reinforcement on the confined strength of concrete was included in confinement index. [4] and [5] considered spacing of transverse stirrups more than the least dimension of the column section as ineffective and calibrated coefficient C_i of their proposed model by using data of experiments carried out on 150 mm × 300 mm concrete cylinder. [6, 7] carried out number of experiments on 150 mm x 300 mm cylinders cast with varied strength of concrete and confined by varied diameter and yield strength of spiral transverse reinforcement. A large scatter was found between results of regression analysis performed on the experimental data and that obtained by using confinement index C_i proposed by [4]. Watanabe et al. [8] suggested a confining coefficient

using the ratio of original core volume and that defined as effectively confined core. The limit strain given by the proposed model was found to be conservative. [9,10] conducted experiments on axial loaded circular columns with 500 mm diameters and 1500 mm height. The specimens were reinforced by 8 to 36 longitudinal reinforcement bars and confined with transverse reinforcement with varied spacing and yield strength. The test results and equation given by [11] was used to suggest a model in form of a fractional equation to estimate the confined compressive strength of concrete. The model catered for effect of volume of effectively confined core and configuration of lateral and longitudinal reinforcement through confining coefficient and effective lateral confining stress. The comparison of results of model with experimental data indicated that its estimates were normally on higher side. It was found that higher strength transverse reinforcement required higher axial compression to develop effective confining pressure. [12] and [13] found that initial strength enhancement due to rectangular hoops was negligible. Later [14] found evident strength enhancement by introducing cross ties in four prototype reinforced concrete columns. [14] modified the basic model proposed by [15] and included the effect of cross ties in the strength enhancement due to rectangular hoops. [16] introduced an effectiveness factor which utilized the configuration and spacing of both longitudinal and transverse reinforcement. The model of [16] was modified by [17] in the same year. [18] presented a model which related the strength and deformability to confinement. The confinement efficiency coefficient used by [18] was later modified to a simpler version [19, 20]. [21] developed a model for bridge piers using their indigenous experimental data. The results of Hoshikuma et al. model are conservative because it does not incorporate effects of configuration of longitudinal and transverse reinforcement. [22] proposed a fractional equation which incorporated effect of spacing and configuration of confining and longitudinal reinforcement on strength and strain through separate efficiency coefficient and volumetric ratio " $\rho_{s\theta}$ ". [23] defined the stress-strain curve for confined concrete. They used Popovic's [11] equation for ascending portion of the curve, [24] equation for

sustaining part and presented a new equation for descending branch of the curve.

In the confinement models the effects of configuration and spacing of longitudinal and transverse reinforcement have been realized and included through an efficiency coefficient. The basic argument used in modelling indicates that stress-strain behaviour of confined concrete is dependent on effective confinement pressure, peak stress, peak strain and deteriorating rate. The estimation of the peak compressive stress of the confined concrete presented by the models was representable, however, conservation is observed in estimation of peak strain. The stress-strain curves of confined concrete have significant role to play in inelastic seismic response of RC multistorey building structures and thus economizing over the seismic design. Therefore, efforts are continuous to estimate the stress-strain curves of confined concrete while considering different confining configuration and material strengths. Effect of configuration and spacing on the compressive strength of confined concrete was the motivation for the authors to propose a confining technique. The proposed technique has been tested in an extensive experimental work consisting of eight prototype column specimens. Four column specimens were confined with proposed technique and four with standard stirrups. The concrete strength was varied to study its effects on proposed confining technique. In this paper data of three columns confined with standard stirrups and cast with different concrete strengths is being presented. Experimentally studied load-displacement relation of these columns is estimated using a simple technique, which use the section analysis of Response-2000 [25] as input. The authors apprehend that the technique will be useful for the reader, who might use any other appropriate software to generate the required input data. The techniques are presented in the form of algorithms which can be easily implemented. The comparison of the proposed technique with studied experimental response is found in good agreement. The authors are presenting the proposed technique with a view that its linear variation approach predicts post peak behaviour better than existing Axial-Shear-Flexure Interaction schemes.

2. Modeling on Response-2000

Moment-Curvature ($M-\phi$) and Shear Force-Shear Strain ($V-\gamma$) relations can be produced using Modified Compression Field Theory [26]. Response-2000 relates variation in stresses and strains using the theory [27]. The program assumes that rate of flexural stresses across a section defines shear stresses [28] and generates a load-displacement response by using its member response function. When the curves generated by member response function were compared with those studied in the lab, the former were found deficient in estimating ultimate displacement for the actual columns. This is because Modified Compression Field Theory is force-based and does not work beyond the peak strength [29]. Therefore, two different approaches have been suggested here in this paper.

2.1 Approaches to Plot Theoretical Load Displacement Curves

The push-over curve of a column, cut at its point of inflection, under application of a load vector “P” and constant axial load “N” can be calculated by summing the contribution of flexure and shear strain to the total displacement “ Δ ” at “B” as marked in Figure 1. Figure 1 is mathematically represented in equation 1. The curvature ϕ_i and shear strain γ_i can be determined from Response-2000.

$$\Delta = \sum_{i=1}^n [\phi_i d_i x_i + \gamma_i d_i] \quad (1)$$

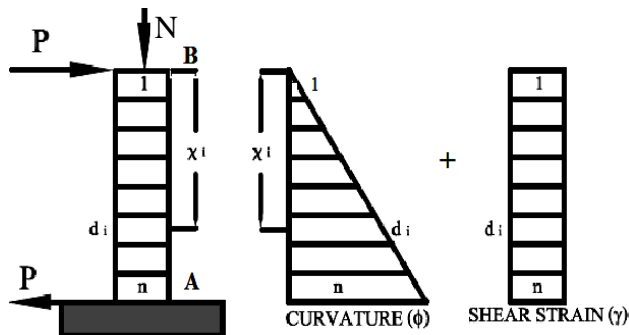


Fig.1 Flexure and shear components of deflection under a lateral load vector “P” and axial load “N”

In the present study, the curvature and shear strain achieved from Response-2000 have been used in two different procedures named as linear variation and interpolation approach to determine displacement

“ Δ ” of equation 1. These procedures have been compared with the experimental results and member response of Response-2000.

2.1.1 Linear Variation Approach

The $M-\phi$ and $V-\gamma$ plots, given by Response-2000, cater for full inelasticity. The shear dominant section is located at $0.9d$ from the support, whereas, maximum moment is considered at the face of the support of the column element [26]. The critical section can be determined by comparing their respective peak loads. In this approach analysis on response-2000 is carried out for critical section only. It is assumed that deformations in a column element, which has been cut at the point of inflection, are concentrated at critical section and vary linearly along the length of the element. The procedure is listed below:

- i. Analyse shear and moment dominant sections and plot $V-\gamma$ and $M-\phi$ relationships respectively using Response-2000.
- ii. Compare the peak loads of the sections and declare the section failing at lower load as critical.
- iii. Determined Load vector of moment-curvature relationship of Response-2000.
- iv. Divide the column in to “n” number of strips of equal height “d”.
- v. Three vectors i.e force “P”, curvature “ ϕ ” and shear strain “ γ ”, derived from $M-\phi$ and $V-\gamma$ relationship of critical section, are used to determine the load-displacement curve for the column. For any value “Pi” of load vector “P” there will be corresponding value of curvature Φ_i and shear strain γ_i of vectors “ Φ ” and “ Γ ” respectively. In curvature ϕ_{ni} and shear strain γ_{ni} , shown in Figure 2, the subscript “n” and “i” indicates that these correspond to n^{th} strip of the column and i^{th} element of vector “ Φ ” and “ Γ ” respectively. The subscript “i” also indicates that Pi is the corresponding element of load vector “P”.
- vi. The curvature ϕ_{ni} is varied linearly while ϕ_{ni} remain constant over the length of the column. In Figure 2, ϕ_{ji} and ϕ_{ji} are curvature and shear strain, corresponding to i^{th} element of vectors

“ Φ ” and “ Γ ” respectively, of j^{th} strip of the column.

- vi. The curvature is assumed to remain constant for entire height “ d ” of the element.
- vii. The curvature of the j^{th} strip is calculated as $\phi_{ji} = (\phi_{ni} / x_n) x_j$.
- viii. Flexure contribution of j^{th} strip to “ Δ_i ” corresponding to “ P_i ” is given as $\phi_{ji} x_{ji} d$.
- ix. The shear strain of J^{th} is $\gamma_{ji} = \gamma_{ni}$ and its contribution to “ Δ_i ” is $\gamma_{ni} d$.
- x. Total contribution of j^{th} strip to “ Δ_i ” under load P_i is given by $\phi_{ji} x_{ji} d + \gamma_{ni} d$.
- xi. Deflection “ Δ_i ” corresponding to load P_i is determined by integrating contribution of strips. This can be represented as equation 2.

$$\Delta_i = \phi_{ni} x_{ni} d + \gamma_{ni} d + \dots + \phi_{ji} x_{ji} d + \gamma_{ni} d + \dots + \phi_{1i} x_{1i} d + \gamma_{ni} d \quad (2)$$

- xii. Change the value of ϕ_i and γ_i for next value of P_i of the load vector and determine the complete load deflection curve.
- xiii. In cases where shear section is critical the values of ϕ_i are determined by linearly extending curvatures of critical section to the base. The shear strain γ_i is considered constant at the face of the support.

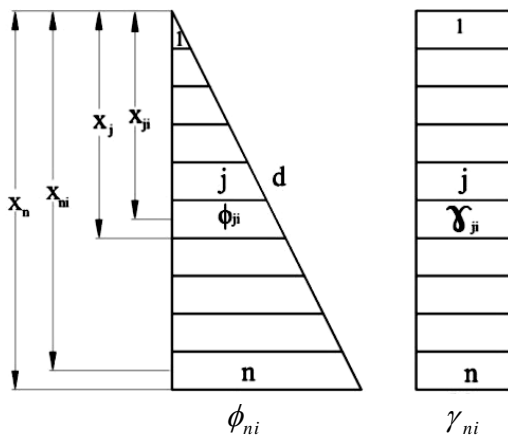


Fig.2 Graphical representation of linear variation approach

2.1.2 Interpolation Approach

In this approach it is assumed that deformation in a column, as shown in Figure 1, is concentrated at critical section and its variation, along the length, depends on $M-\phi$ and $V-\gamma$ relationship of different sections. In this approach curvature and shear strain for each strip, at given load step, are found by interpolating in $M-\phi$ and $V-\gamma$ relationship of a section existing in the mid of that strip. The procedure is explained below.

- i. Find the critical section, as is done in linear variation approach.
- ii. The force vector “ P ” is achieved from analysis of critical section.
- iii. Divide the load vector into two branches i.e., ascending up to peak load and descending from peak till ultimate load.
- iv. Divide the column into “ n ” strips of thickness “ d ”.
- v. For each strip carryout the analysis on Response-2000 i.e., if you have “ n ” strips of thickness “ d ”, there will be “ n ” analysis. Therefore, there will be “ n ” $M-\phi$ and $V-\gamma$ relationships.
- vi. Drive load vector from analysed $M-\phi$ and $V-\gamma$ relationship of each strip so that there are “ n ” load vectors “ p_n ”, where “ n ” represent the number of strip. The maximum and minimum load of each load vector is denoted by p_{\max} and p_{\min} . Similar to load vector “ P ” divide each “ p_n ” and corresponding “ Φ_n ” and “ Γ_n ” into two branches.
- vii. At any load step “ P_i ” of load vector “ P ”, if $p_{\max} \geq P_i \geq p_{\min}$, search in each load vector “ p_n ” for value “ p_{ni} ” equal to “ P_i ”. If value “ p_{ni} ” is not found, then interpolation within load vector “ p_n ” will be adopted. Similarly, corresponding value of curvature ϕ_{ni} and shear strain γ_{ni} will be found, for each strip, in vectors “ Φ_n ” and “ Γ_n ”. Subscript “ n ” and “ i ” represents number of strip and load step of the load vector “ P ”.
- viii. In step “vi” above “ P_i ”, “ p_{ni} ”, Φ_{ni} and γ_{ni} referred to same branch i.e ascending or descending.

- ix. The contribution of any strip, for which $p_{max} < P_i$ or $P_i < p_{min}$, is considered as negligible and is ignored.
- x. Mathematically the displacement “ Δ_i ” for load “ P_i ” is given by equation 2 above. In the equation ϕ_{ni} , ϕ_{ji} and ϕ_{li} and γ_{ni} , γ_{ji} and γ_{ly} are the curvatures and shear strains for n^{th} , j^{th} and l^{st} strip corresponding to P_i and x_n , x_j and x_l are respective moment arms of strips. The thickness of the strip is represented by “ d ”.
- xi. Graphically it is also presented by Figure 2 but difference is in ϕ_{ni} and γ_{ni} as described in step “v” above.

3. Experimental Work

The suggested techniques have been applied to the studied response of RC columns tested under application of constant axial and static cyclic lateral force. The effect of concrete compressive strength on the response of columns has been taken into account through material properties assigned to respective sections in response-2000.

3.1 Specimen and Loading

The detail of test specimen is summarized in Table 1. The transverse reinforcement is provided according to provision of ACI-318-08. Two columns cast with 25 MPa concrete were confined with 415 and 275 MPa transverse reinforcement. The column cast with 32 MPa concrete was confined with 415 MPa concrete. The dimensions of shear block, provided with the column, were enough to ensure that there is no contribution of the base to the response of the column. In the first cycle 0.25% drift level was applied. In the second cycle it was increased to 0.5%. After second cycle each drift level was repeated once to ensure that response of column at each drift level is thoroughly studied. An increment of 0.5% in drift

levels was adopted up to 5% drift level. At 5% the increment was reduced to 0.25%. The final drift level of 5.5% was repeated until 20% degradation in strength was achieved. Throughout the test the axial load was monitored and variation of 7 to 10% has been observed. The nomenclature assigned to columns is listed in Table 1. In the Table 1 CRCS represents Conventionally Reinforced Concrete Stirrup.

3.2 Testing Arrangement

Standard test assembly for static cyclic loading was used as shown in Figure 3. In order to include details two views, from different angles, has been combined in Figure 3. The shear block was anchored on the strong floor. The axial load was applied through bridge roller assembly which ensured application of lateral and axial loads simultaneously without any unnecessary restraint. The axial and lateral loads were applied through different assembly of shear frames so that the effect of one loading does not influence the other. The test setup is shown in Figure 3 and its details are also given.

3.3 Instrumentation

The displacements were measured by means of LVDTs installed at 1734 mm, 515.5 mm and 169 mm from shear block. These locations represented full, hinge and shear depth of the specimen. Three steel strain gages were installed to measure strain variation of two longitudinal and one transverse reinforcement bar within the hinge zone. The force acting on the balance rods of bridge roller assembly was calculated from recorded strains and subtracted from lateral loads applied. All the loads were measured through load cells. All the gages and load cells were attached to Strain Smart-5000 scanner. The instrumentation is shown in Figure 4 and its details are given in Table 2.

Table 1 Specimen geometry, reinforcement, material properties and applied load

Column Index	Column Size (mm)	Column Size (mm)	Concrete strength (MPa)	Longitudinal steel (mm) 415 MPa	Transverse steel Size (mm), f_t (MPa)	Hinge length (l_o) (mm)	Spacing lateral (within l_o) (mm)	Spacing lateral(out of l_o) (mm)	Axial Load (kN)	Transverse Load
CRCS-60-25	230x230	1734	25	8#12	10, 415	515.5	57	76	132.25	Static cyclic
CRCS-40-25	230x230	1734	25	8#12	10, 275	515.5	57	76	132.25	Static cyclic
CRCS-60-32	230x230	1734	32	8#12	10,415	515.5	57	76	169.28	Static cyclic

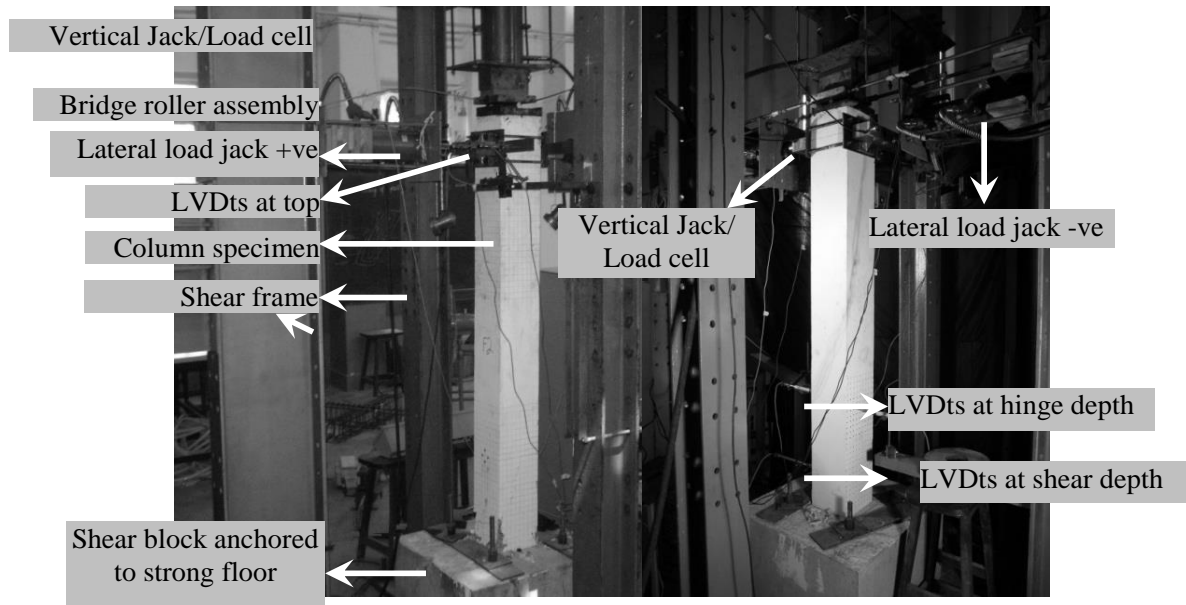


Fig. 3 General layout of the setup used in testing of RC column specimens

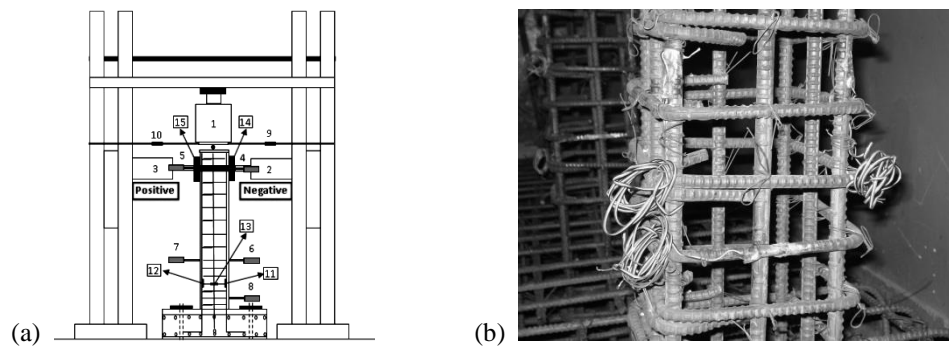


Fig.4 (a) Line diagram of test setup indicating instrumentation installed to record response of column specimen
(b) Linear strain gages installed on longitudinal and transverse reinforcement

Table 2 Detail of instrumentation as marked in line diagram of Figure4

Serial	Instruments and Their Location
1	Axial load jack
2 & 3	Lateral load jack for negative and positive direction of loading
4 to 8	LVDT at top, hinge depth and shear depth to measure lateral displacement
9 & 10	Pair of steel strain gages measuring strain of balancing rods for negative direction
11 to 13	Steel strain gage measuring strain of longitudinal and transverse steel bar
14 & 15	Load cell measuring lateral load in positive and negative direction

Each column was tested up to degradation level of 20%. Only data of LVDTs located at top of the columns is being presented and analysed in this paper. In observed behaviour of columns the positive loading direction is always found dominating because each displacement level is negotiated for the first time in that direction and it is always a non-damaged state. Major damage in all columns has been observed within the hinge zone depth.

3.4.1 Testing of CRCS-60-25

The 20% degradation was achieved in 27 cycles. The deformation in the column started in 2nd cycle. The damage in the column was observed up to 592 mm depth. Final damage observed in the column is shown in Figure 5(a) and 5(b). The peak load of

31.48 kN occurred at 2.98% drift level. The spalling of cover for both directions started at 4.5% drift level. The hysteresis response of the column is plotted in Figure 6(a) and its backbone curve overlapped with smoothed curve is given in Figure 6(b).

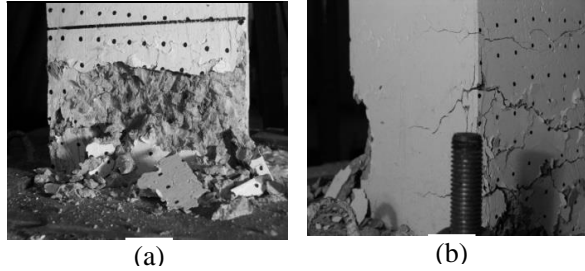


Fig.5 Final damage observed in CRCS-60-25 column cast with 25 MPa concrete (a) positive loading face (b) Negative loading face

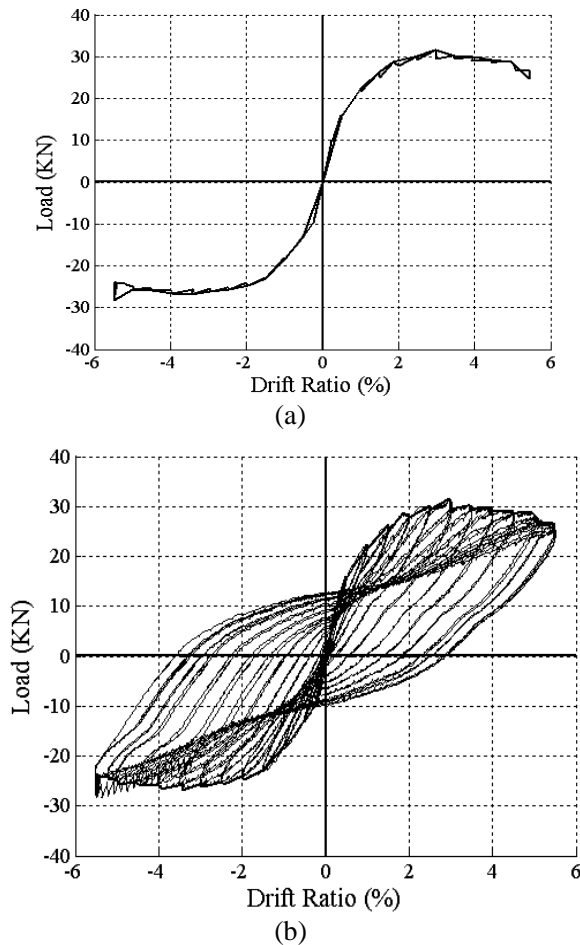


Fig.6 Load-displacement curves of CRCS-60-25 cast with 25 MPa concrete (a) Backbone curves marked on hysteresis curves (b) Actual and smoothed backbone curves

3.4.2 CRCS-40-25

Total 29 cycles were applied to the column in order to achieve 20% strength degradation. First crack appeared at a lateral displacement of 5.5 mm. The peak load of 29.89 kN occurred in the positive direction at 40.22 mm displacement in the 10th cycle. The extent of deformation was noted up to a depth of about 220 mm. The view of the damage of the column is shown in Fig 7(a) and 7(b). The hysteresis curve of cyclic test of column is shown in Figure 8(a) and its backbone curve overlapped with smoothed curve is shown in Figure 8(b).

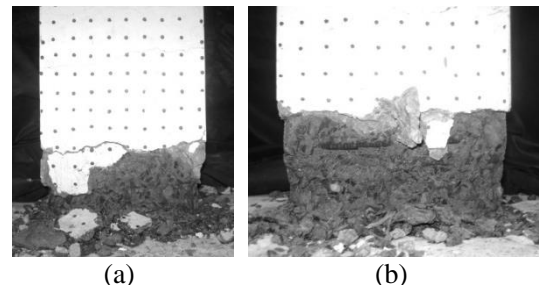


Fig.7 Final damage observed in CRCS-40-25 column cast with 25 MPa concrete (a) positive loading face (b) Negative loading face

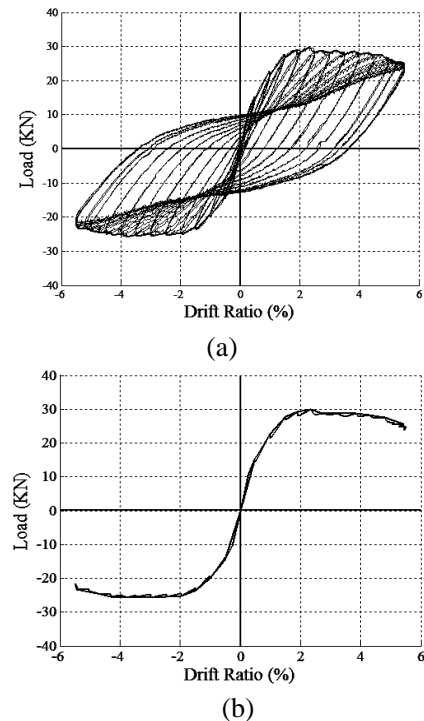


Fig.8 Load-displacement curves of CRCS-40-25 cast with 25 MPa concrete (a) Backbone curve marked on hysteresis curves (b) Actual and smoothed backbone curves

3.4.3 CRCS-60-32

In the loading cycles, applied during testing, an increment of 1% drift level was monitored. However, the results were found comparable with other columns. The first crack on the positive face appeared at a lateral displacement of 8.2 mm. The damage in the column appeared up to a depth of 790 mm. The peak load was noted as 34.09 kN occurring at 2.85% drift level. The spalling was initiated at lateral displacement of 65 mm and aggravated at 72 mm. The required 20% degradation in strength was achieved in 15 cycles. The damage observed in the column is shown in Figures 9(a) and 9(b). The hysteresis curve is given in Figure10(a) and its backbone curve, overlapped with smoothed curve, is shown in Figure10(b).

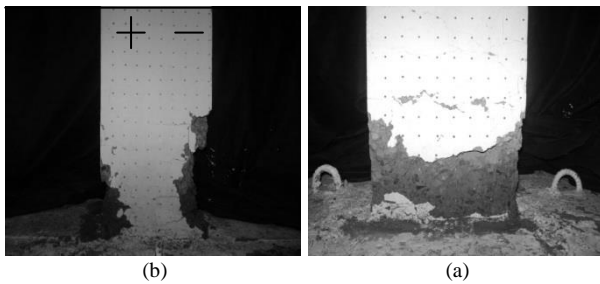


Fig.9 Final damage observed in CRCS-60-32 column cast with 32 MPa concrete (a) positive loading face (b) Negative loading face

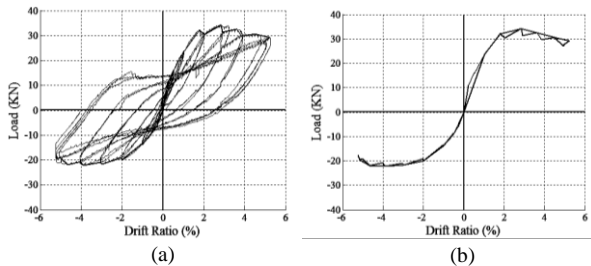


Fig.10 Load-displacement curves of CRCS-60-32 cast with 32 MPa concrete (a) Backbone curve marked on hysteresis curves (b) Actual and smoothed backbone curves

4. Estimation load-displacement backbone curves using Response-2000

The two approaches are applied on CRCS-60-25, CRCS-40-25 and CRCS-60-32 columns. The analytical curves do not capture strain penetration

and pinching in the negative direction accurately. Therefore, for comparison mean curve of positive and negative backbone curves of experimental load-displacement hysteresis are used. The proposed approaches are also compared with member response of Response-2000. The linear variation approach has shown satisfactory results for estimating the ultimate displacement of the experimental backbone curve. The results of interpolation approach are found almost identical with member response of Response-2000 program.

4.1 CRCS-60-25

The mean backbone curve of the column is plotted in Figure 11. The mean curve has been compared with linear variation and member response of Response-2000 in Figure 12 and 13 respectively. Both the curves have estimated peak lateral force accurately. The estimate of ultimate displacement is 17% and 69% lesser than mean experimental curve. The linear variation and interpolation approaches are compared with member response of Response-2000 in Figure 14 and 15 respectively. The estimate of peak lateral force is same in the three approaches. The ultimate displacement given by linear variation and interpolation is 66% and 13% higher than that achieved from Response-2000. The two suggested approaches are compared in Figure 16. The ultimate displacement of linear variation curve is 69.24% higher than interpolation curve. It is noted that estimated ultimate displacement by linear variation approach is in good agreement with the experimental curve.

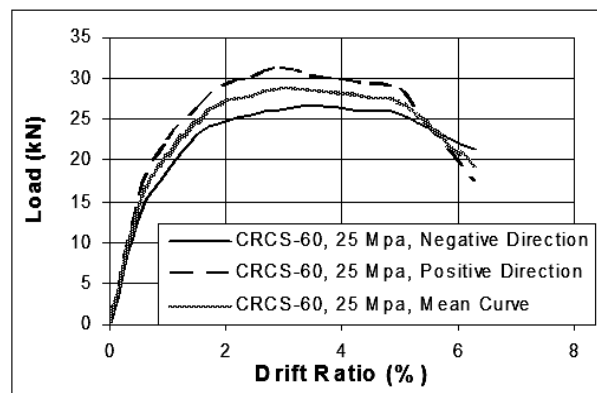


Fig.11 Mean curve of CRCS-60-25 drawn by plotting backbone curves of positive and negative direction in first quadrant

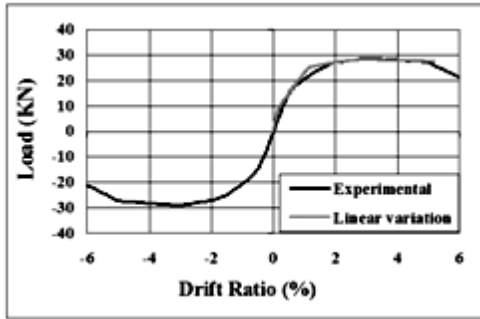


Fig. 12 Experimental and linear variation curves of CRCS-60-25 overlapped

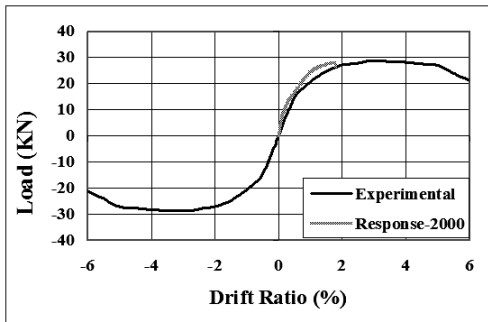


Fig. 13 Experimental and member response curves of CRCS-60-25 overlapped

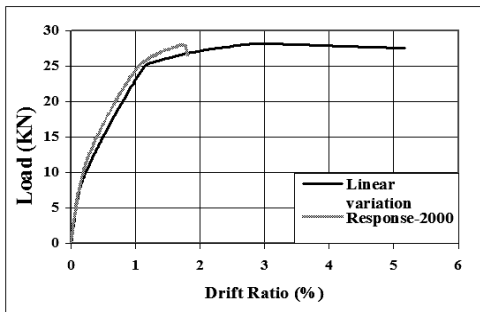


Fig. 14 Linear variation and member response curves of CRCS-60-25 overlapped

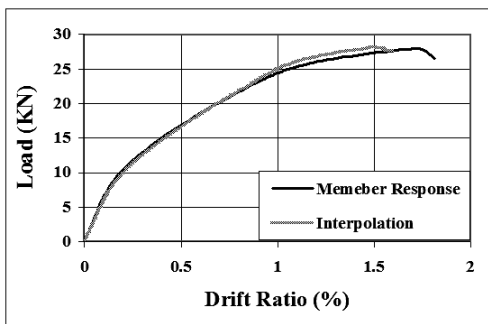


Fig. 15 Member response and interpolation curves of CRCS-60-25 overlapped

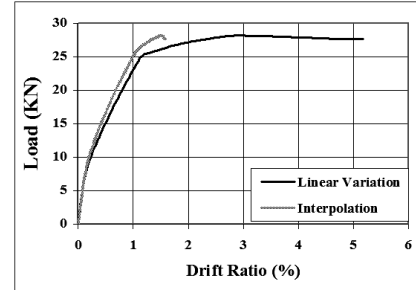


Fig. 16 Linear variation and interpolation curves of CRCS-60-25 overlapped

4.2 CRCS-40-25

The backbone curves, in negative and positive direction, of CRCS-40-25 have been plotted in first quadrant and their mean is drawn in Figure 17. The peak lateral load estimated by all approaches, for CRCS-40-25 column, is approximately equal and closely matches the value of peak load of mean experimental curve. The ultimate displacement estimated by linear variation approach is 20.21% lesser than mean experimental curve, shown in Figure 18. The Response-2000 curve has under estimated ultimate displacement by 72% plotted in Figure 19. The linear variation and interpolation approach has been compared with Response-2000 curve in Figure 20 and 21. The estimate of ultimate displacement of interpolation and linear variation approach is 12.6% and 64.7% higher than the value given by Response curve. The linear variation and interpolation approach has been compared with each other in Figure 22. The ultimate displacement of linear variation curve is 69.4% higher than interpolation curve. Comparison carried out here dictates that estimate of linear variation approach has been more realistic due to its accuracy in calculation of ultimate displacement.

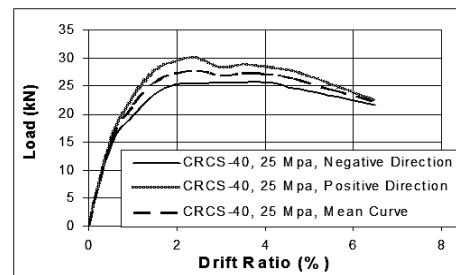


Fig. 17 Mean curve of CRCS-40-25 drawn by plotting backbone curves of positive and negative direction in first quadrant

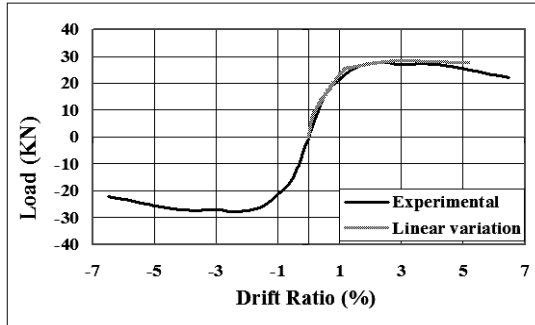


Fig. 18 Experimental and linear variation curves of CRCS-40-25 overlapped

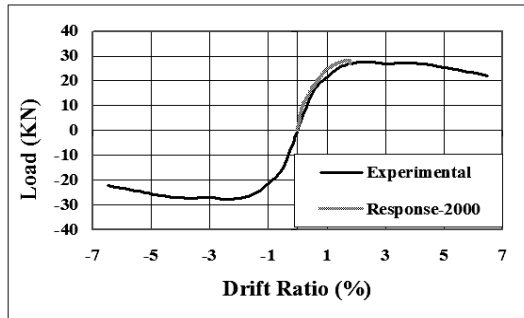


Fig. 19 Experimental and member response curves of CRCS-40-25 overlapped

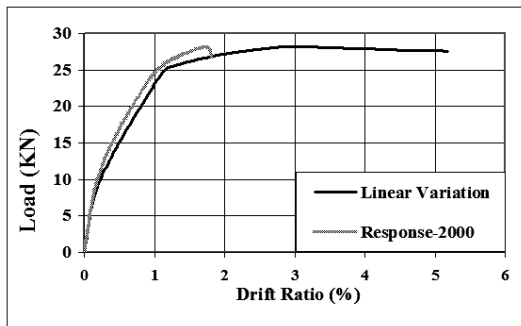


Fig. 20 Linear variation and member response curves of CRCS-40-25 overlapped

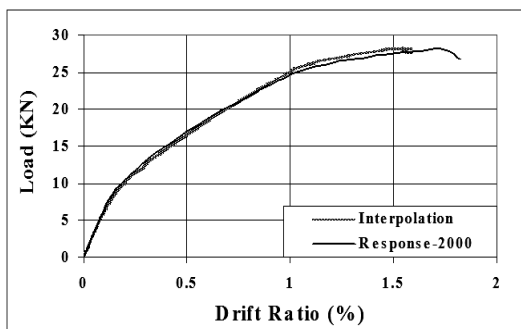


Fig. 21 Member response and interpolation curves of CRCS-40-25 overlapped

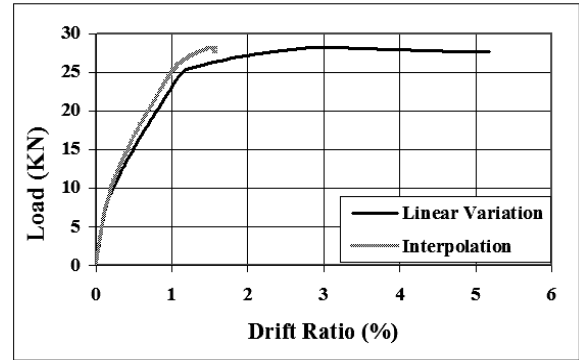


Fig. 22 Linear variation and interpolation curves of CRCS-40-25 overlapped

4.3 CRCS-60-25

The backbone curves of load-displacement hysteresis for positive and negative direction are plotted in first quadrant in Figure 23 and the mean curve is drawn. The linear variation approach is overlapped with experimental mean curve in Figure 24. The theoretical curve has over estimated load displacement response which is obvious because it is difficult to capture strain penetration accurately. The estimated peak load is 10% higher than that of mean curve. The linear variation approach has estimated ultimate displacement quite accurately. The member response of Response-2000 is overlapped with the mean curve in Figure 25. The lateral force of Response-2000 curve is 10% higher but it has estimated 66% lesser ultimate displacement. In Figure 26 linear variation approach is overlapped with member response curve of Response-2000. The response curve has higher initial slope but its estimate of peak lateral force is same as that of linear variation approach. The member response of Response-2000 and interpolation approach has been plotted together in Figure 27. Both curves has followed almost same path but interpolation approach has estimated 27% larger ultimate displacement than member response of Response-2000. In Figure 28 linear variation and interpolation approach has been superimposed. The estimate of peak lateral force is again same but ultimate displacement of linear variation approach is 57% higher than interpolation approach. Similar, level of lateral force has been estimated by all approaches but ultimate displacement has been estimated accurately by linear variation approach only.

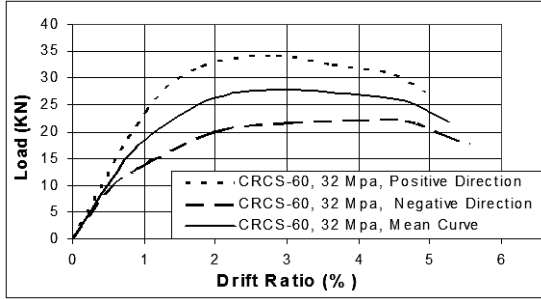


Fig. 23 Mean curve of CRCS-60-32 Mpa concrete drawn by plotting backbone curves of positive and negative direction in first quadrant

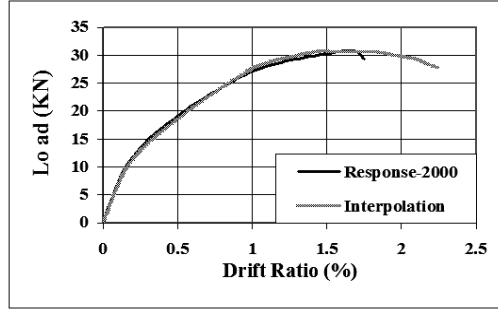


Fig. 27 Interpolation and member response curves of CRCS-60-32 overlapped

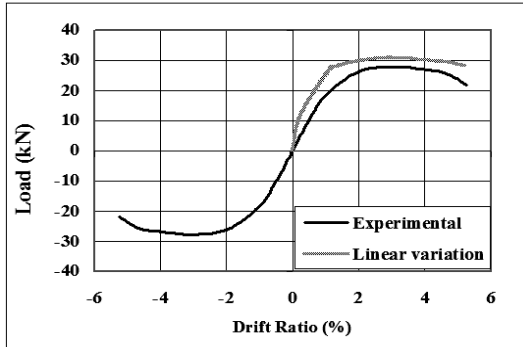


Fig. 24 Experimental and linear variation curves of CRCS-60-32 overlapped

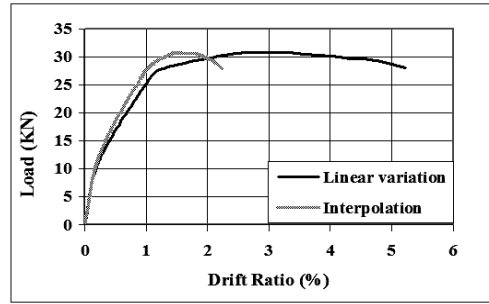


Fig. 28 Linear variation and interpolation curves of CRCS-60-32 overlapped

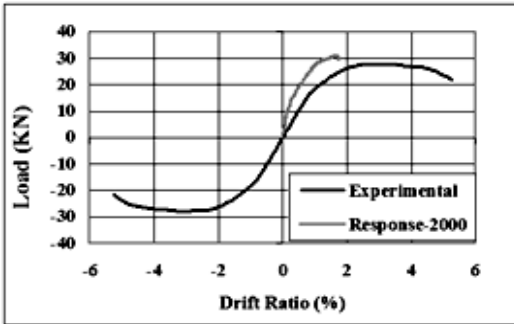


Fig. 25 Experimental and member response curves of CRCS-60-32 overlapped

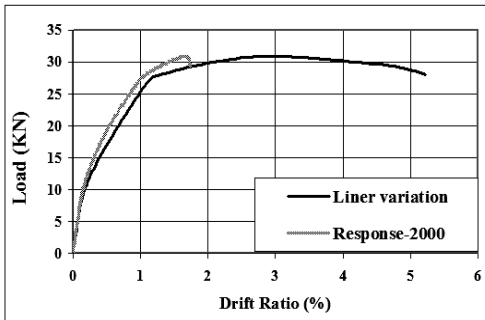


Fig. 26 Linear variation and member response curves of CRCS-60-32 overlapped

5. Limitation

The approaches are applicable for unidirectional lateral and constant axial load cases. The response of RC columns is affected with pattern of loading. The approaches cannot address the complexity involved in combing moment-curvature relation of two orthogonal directions.

6. Conclusions

The use of mean experimental curves catered for any short fall which may be present in experimental setup. Mostly, hysteresis plotted by analytical procedure has similar properties in both positive and negative direction. The use of mean of backbone curve of positive and negative directions has accommodated limitation of analytical procedures. Estimate of ultimate displacement of load-displacement curves by response-2000 has been much conservative. The estimation of load-displacement curves of RC columns by interpolation approach approximately matches member response option of response-2000. The load-displacement curves estimated by linear variation approach were found closest to the mean experimental curves.

7. Acknowledgement

The authors acknowledge the support of Pakistan Higher Education Commission, Islamabad for funding this research work.

References

- [1] Sheikh S A, 1978. Effectiveness of Rectangular Ties as Confinement Steel in Reinforced Concrete Columns.” Ph.D Thesis, Department of Civil Engineering, University of Toronto, Canada, pp. 256.
- [2] Richart, F. E., Brandzaeg, A. and Brown, R. L. 1928. “A study of the failure of concrete under Combined Compressive Stresses”. University of Illinois Engineering Station, Bulletin No. 185, 104 pp.
- [3] Balmer, G.G. 1943. “Shearing Strength of Concrete under High Triaxial Stresses – Computation of Mohr’s Envelope as a Curve”. Structural Research Laboratory Report No. SP-23, U.S. Bureau of Reclamation, 13 pp. plus tables and Figures.
- [4] Iyengar, S.R., Desayi, K.P.T., and Nagi, R.K.; Desayi and Nagi Reddy, K., 1970. “Stress-Strain Characteristics of concrete Confined in Steel Binder”, Magazine of Concrete Research, Vol. 22, No 72, pp. 173-184.
- [5] Parakash Desayi, Sundara Raja Iyengar, K.T. and Sanjeeva Reddy, T. 1978. “Equation for Stress-Strain Curve of Concrete Confined in Circular Steel Spiral”, Matériau et Constructions, Vol. 11 – No 65, pp. 339-345.
- [6] Muguruma, H., Watanabe, F., Tanaka, H., Sakurai, K. and Nakamura, E. 1979. “Effect of Confinement by High Yield Strength Hoop Reinforcement upon the Compressive Ductility of Concrete”, Proceedings of the Twenty-Second Japan Congress on Material Research, The Society of Material Science, Japan, pp. 377-382.
- [7] Muguruma, H., Watanabe, F., Tanaka, H., Sakurai, K. and Nakamura, E. 1979. “Study on Improving the Flexure and Shear Deformation Capacity of Concrete Member by Using Lateral Confining Reinforcement with High Yield Strength”, Comité Euro-International du Béton, BULLETIN D'INFORMATION No 132, Volume 2 – Technical Papers, AICAP-CEB Symposium, Rome, May, pp. 37-44.
- [8] Watanabe, F., Muguruma, H., Tanaka, H. and Katsuda, S., 1980. “Improving the Flexural Ductility of Prestressed Concrete Beam by Using the High Yield Strength Lateral Hoop Reinforcement”, FIP, Symposia on Partial Prestressing and Practical Construction in Prestressed and Reinforced Concrete, Proceedings: Part 2, Bucuresti-România, pp. 398-406.
- [9] Mander, J. B., Priestley, M.J.N. and Park, R. 1988. “Theoretical Stress Strain Model for Confined Concrete” Journal of Structural Engineering, American Society of Civil Engineers, vol. 114, No. 8, pp. 1804-1826.
- [10] Mander, J. B., Priestley, M.J.N. and Park, R. 1988. “Observed Stress-Strain Behavior of Confined Concrete” Journal of Structural Engineering, American Society of Civil Engineers, No. 8, pp. 1827-1849.
- [11] Popovics, S. 1973. “A Numerical Approach to the complete Stress-Strain Curves of Concrete”, Cement and Concrete Research, Vol. 3, No. 5, pp. 583-599.
- [12] Roy, H.E.H. and Sozen, M.A. 1964. “Ductility of Concrete”, Proceedings of the International Symposium on Flexural Mechanics of Reinforced Concrete, ASCE-ACI, Miami, pp. 213-224.
- [13] Soliman, S.A. and Uzumeri, S.M., 1979. “Properties of Concrete Confined by Rectangular Tie”, AICAP-CEB Symposium on Structural Concrete under Seismic Actions (Rome, May 1979), Bulletin d'Information No. 132, Comité Euro-International du Beton, Paris, pp-53-60.
- [14] Park, R., Priestley, M.J.N. and W.D. Gill. 1982. “Ductility of Square Confined Concrete Columns” Proceedings ASCE, Vol. 108, ST4, pp-929-950.

- [15] Kent, D. C. and Park, R. 1971. "Flexural Members with Confined Concrete", Proceedings of ASCE, Vol. 97, No. ST 7, pp. 1969-1990.
- [16] Sheikh S. A. and Uzumeri, S. M., 1980. "Strength and ductility of tied concrete columns", Journal of the structure division, ASCE, 106(5), pp 1079-1102.
- [17] Sheikh S. A. and Yeh C.C., 1982. "Flexural behavior of confined concrete columns", ACI Journal, pp-389-404.
- [18] Saatcioglu, M. and Razvi, S. R., 1992. "Strength and ductility of confined concrete", Journal of Structural Engineering, ASCE, 118 (6), pp. 1590-1607.
- [19] Razvi, S. R. and Saatcioglu, M. 1996. "Design of RC columns for confinement based on lateral drift", Ottawa-Carleton Earthquake Engineering Research Center, Report OCEERC 96-02, Dept. of Civil Engineering, Univ. of Ottawa, Ottawa, Canada, pp. 92.
- [20] Razvi, S. R. and Saatcioglu, M. 1999. "Stress-strain relationship for confined high strength concrete", Journal of Structural Engineering, ASCE, 125 (3).
- [21] Hoshikuma, J., Kawashima, K., Nayaga, K. and Taylor, A.W. 1994. "Stress-strain model for confined RC in bridge piers", Journal of Structural Engineering, Vol.123(5), pp-624-633.
- [22] EL-Dash. K. M. and Ahmad. S. H. 1994. "A model for the stress-strain relationship of rectangular confined normal and high strength concrete columns", Material and structures, No. 27, pages 572-579.
- [23] Bousalem, B. and Chikh, N. 2006. "Development of a confined model for rectangular ordinary reinforced concrete columns", Journal of Material and Structures, DOI 10.1617/s11527-06-9172-2.
- [24] Bing, L., Park, R. and Tanaka, H. 2001. Stress-strain behavior of high strength concrete confined by ultra-high and normal strength transverse reinforcements. Structural Journal, ACI, May-June, pp-395-406.
- [25] Response 2000. 2013. "A sectional analysis program that will calculate the strength and ductility of a reinforced concrete cross-section subjected to shear, moment, and axial load" <http://www.ecf.utoronto.ca/~bentz/r2k.htm>, last visited on August 2013.
- [26] Vecchio F.J and Collins M. P 1988. "Predicting the response of reinforced concrete beams subjected to shear using modified compression field theory". ACI Structural Journal, Vol 85 No 3, pp-258-268.
- [27] Bentz E. C. and Collins M. P 2009. "Load-Deformation Response of Reinforced Concrete Sections". <http://www.ecf.utoronto.ca/~bentz/inter4/inter4.shtml>, Visited on 19 March 2013.
- [28] Bentz E. 2001. "Response 2000, Shell 2000, Triax 2000 and Membrane 2000", User Manual. Version 1.1.
- [29] Shi-Yu Xu and Jian Zhang., 2008. "Hysteresis Models for Reinforced Concrete Columns Considering Axial-Shear-Flexure Interaction". The 14th World Conference on Earthquake Engineering October 12-17, Beijing, China.